Electronic Supplementary Material (ESI) for Journal of Materials Chemistry C.

Construction fully carbon-based fillers with hierarchical structure to fabricate highly thermally conductive polyimide nanocomposites

Yongqiang Guo[1], Kunpeng Ruan[1], Xutong Yang[1], Tengbo Ma[1],

Jie Kong[1], Nannan Wu[3,4], Jiaoxia Zhang,[3,5] Junwei Gu[1,2]*, Zhanhu Guo[3*]

[1] MOE Key Laboratory of Material Physics and Chemistry under Extraordinary Conditions, Shaanxi Key Laboratory of Macromolecular Science and Technology, Department of Applied Chemistry, School of Science, Northwestern Polytechnical University, Xi' an, Shaanxi, 710072, P.R. China.

[2] State Key Laboratory of Solid Lubrication, Lanzhou Institute of Chemical Physics, Chinese Academy of Sciences, Lanzhou, 730000, P. R. China.

[3] Integrated Composites Laboratory (ICL), Department of Chemical & Biomolecular Engineering, University of Tennessee, Knoxville, TN 37996, USA.

[4] National Engineering Research Center for Advanced Polymer Processing Technology, Zhengzhou University, Zhengzhou, 450002, China

[5] School of Materials Science and Engineering, Jiangsu University of Science and Technology, Zhenjiang 212003, China

*Corresponding author: E-mail: gjw@nwpu.edu.cn & nwpugjw@163.com (J. Gu); zguo10@utk.edu (Z. Guo)

Theoretical derivation of the thermal conductivity

Traditional thermal conduction models for polymer composites mainly consider the thermal conductivity coefficient (λ) and volume fraction of fillers, usually ignoring the influences of fillers/matrix interfaces, fillers' dispersion and alignment, *etc*. resulting in large discrepancy between theoretical and experimental λ values.

In order to further clarify the synergistic effect of *f*-MWCNT and rGO, and to improve the accuracy of theoretical λ values for *f*-MWCNT-*g*-rGO/PI nanocomposites, an improved thermal conduction model is proposed and optimized, which is based on the effective medium theory (EMT) and heat conservation, considering the fillers/matrix interfaces, fillers' dispersion and alignment, *etc.*

Thermal conductivity measurement (transient plane heat source method) indicates the heat conduction process is unsteady state, and the samples can be seen as one part of the semi-infinite body.[1, 2] According to the Fourier's law,[3] the heat (Q) transferred into the semi-infinite body at a specific time (τ) can be expressed as:

$$Q = F\int_{0}^{\tau} q(0,\tau)d\tau \qquad (Eq.S1)$$

Where, F is isothermal level, a constant when the surface temperature distribution of the semi-infinite body is uniform; $q(0,\tau)$ represents the heat flow that goes through the semi-infinite body and can be expressed as:

$$q(0,\tau) = \frac{\lambda\Delta T}{\sqrt{\pi\alpha\tau}} \qquad (Eq.S2)$$

where, α is the thermal diffusivity; ΔT is the surface temperature change of the semi-infinite body.

Therefore, Q can be expressed as:

$$Q = 2\lambda F \Delta T \sqrt{\frac{\tau \rho c}{\pi \lambda}} \qquad (Eq. S3)$$

where, ρ and c is density and specific heat capacity of the sample, respectively.

According to EMT model, the in-plane and cross-plane thermal conductivity of the polymer composites (**Figure S1a**) can be express as:[4]

$$\lambda_{11}^{*} = \lambda_{22}^{*} = \lambda_m \frac{2 + V_f\left[\frac{\lambda_f}{\lambda_m}\left(1 + \langle \cos^2\theta \rangle\right)\right]}{2 - V_f\left[\left(1 - \frac{R_{Bd}\lambda_m}{h}\right)\left(1 - \langle \cos^2\theta \rangle\right)\right]} \qquad (Eq. S4)$$

$$\lambda_{33}^{*} = \lambda_m \frac{1 + V_f\left[\frac{\lambda_f}{\lambda_m}\left(1 - \langle \cos^2\theta \rangle\right)\right]}{1 - V_f\left[\left(1 - \frac{R_{Bd}\lambda_m}{h}\right)\langle \cos^2\theta \rangle\right]} \qquad (Eq. S5)$$

f-MWCNT-*g*-rGO has anisotropic heat conduction (**Figure S1b**), considering the in-plane and cross-plane thermal conductivity individually, so that Eq. S4 and S5 can be simplified as follows:

$$\lambda^{*} = \lambda_m \frac{2 + V_f\left[\frac{\lambda_f}{\lambda_m}\left(1 + \langle \cos^2\theta \rangle\right)\right]}{2 - V_f\left[\left(1 - \frac{R_{Bd}\lambda_m}{h}\right)\left(1 - \langle \cos^2\theta \rangle\right)\right]} \qquad (Eq. S6)$$

$$\langle \cos^2\theta \rangle = \frac{\int \rho(\theta)\cos^2\theta \sin\theta d\theta}{\int \rho(\theta)\sin\theta d\theta} \qquad (Eq. S7)$$

where, λ_m is the thermal conductivity of PI matrix; λ_f is the testing in-plane ($\lambda_{f\parallel}$) or cross-plane ($\lambda_{f\perp}$) thermal conductivity of *f*-MWCNT-*g*-rGO ($\lambda_{f\parallel} \approx$ 120 W/mK，$\lambda_{f\perp} \approx$ 20 W/mK); V_f is the volume fraction of *f*-MWCNT-*g*-rGO, θ is the angle between the *f*-MWCNT-*g*-rGO plane and the horizontal plane of *f*-MWCNT-*g*-rGO/PI composites; $\rho(\theta)$ is the distribution function; < > represents the spatial average; R_{Bd} is the thermal interface resistance (~ 8×10^{-8} (m^2·K) W^{-1}),[5] h is the average thickness of *f*-MWCNT-*g*-rGO (~ 12 nm).

According to the ellipsoid distribution of thermal conductivity[6] (**Figure S1c**), the geometry constituted by the thermal conductivity is an ellipsoid, where the thermal conductivity is axial length (**Figure S1d**). Assuming the volume of the semi-infinite body, the measured sample is one part of the semi-infinite body, and its in-plane and cross-plane thermal conductivity is $\lambda_{\parallel}^{*}$ and $\lambda_{\perp}^{*}$, so that the heat (Q_1) through the sample can be expressed as:

$$Q_1 = \frac{4\pi\lambda_{\perp}^{*}\lambda_{\parallel}^{*2}}{3V} 2\sqrt{\lambda_{\perp}^{*}} F\Delta T \sqrt{\frac{\tau\rho c}{\pi}} \qquad (Eq. S8)$$

Assuming there is another sample in the semi-infinite body and its in-plane and cross-plane thermal conductivity is the same (λ), so the heat (Q_2) through the sample can be expressed as:

$$Q_2 = \frac{4\pi\lambda^3}{3V} 2\sqrt{\lambda} F\Delta T \sqrt{\frac{\tau\rho c}{\pi}} \qquad (Eq. S9)$$

If $Q_1 = Q_2$, the λ can be expressed as:

$$\lambda = \left(\lambda_{\perp}^{*\,1.5}\lambda_{\parallel}^{*\,2}\right)^{2/7} \qquad (Eq. S10)$$

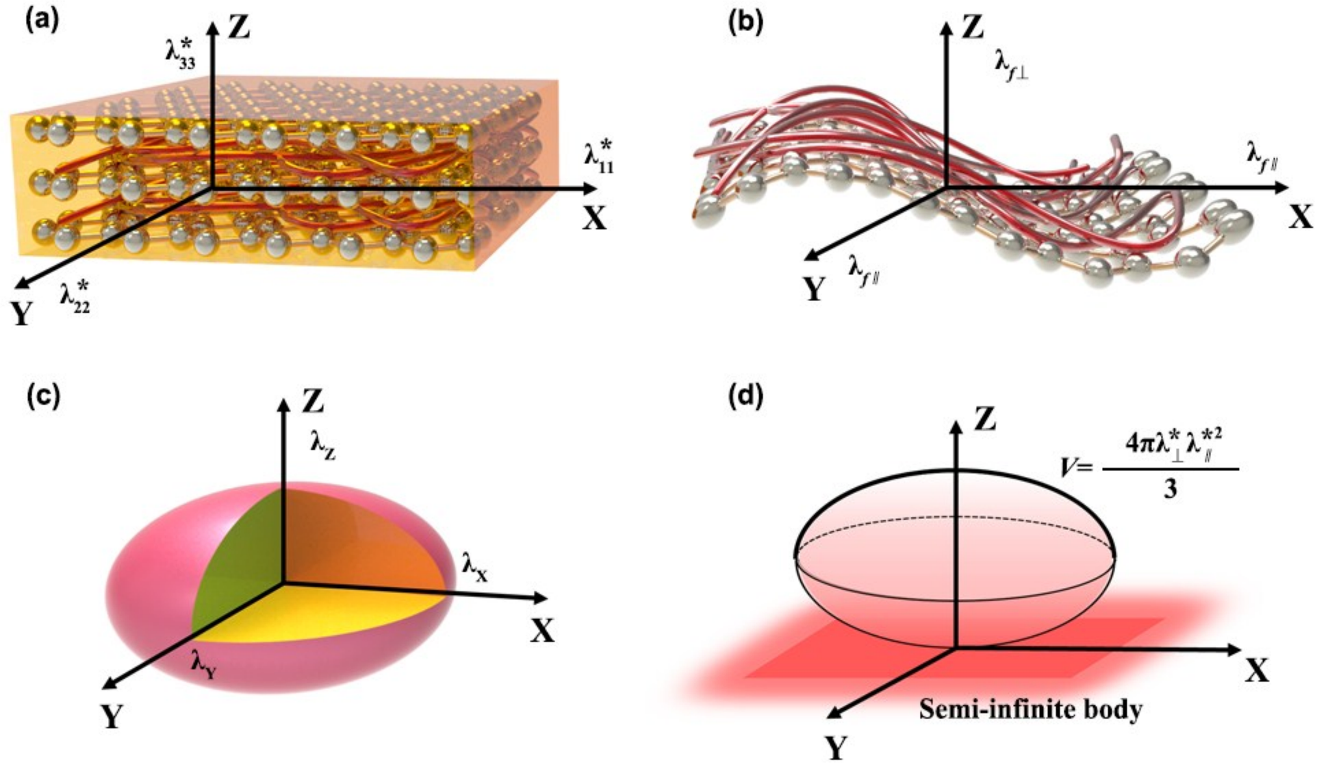

Figure S1 Diagram of the thermal conduction models. (a) Laminate structure of the *f*-MWCNT-*g*-rGO/PI nanocomposites, (b) Anisotropic heat conduction of *f*-MWCNT-*g*-rGO fillers, (c) Thermal conductivity ellipsoid, (d) Heat conduction in semi-infinite body

Table S1 A comparison in λ values for different thermally conductive polymer composites

Fillers' composition & loading	**Polymer matrix**	**λ (W/mK)**	**Enhancement (%)**	**Reference**
10 wt% *f*-MWCNT-*g*-rGO	Polyimide	***1.60***	***490***	***This work***
10 wt% GO-A-CNT	Poly(vinylidene fluoride)	1.56	610	Ref. 7
12.1 wt% CNT-GNPs	Epoxy	0.51	300	Ref. 8
20 wt% MWCNT-GNP	Polycarbonate	1.39	479	Ref. 9
10 wt% CNT-GNP	Poly(vinylidene fluoride)	0.97	260	Ref. 10
13 wt% CNT+GO-MDA	Poly(vinylidene fluoride)	0.39	86	Ref. 11
12 wt% CNT+GO	Poly(vinylidene fluoride)	0.95	270	Ref. 12

Table S2 Characteristic data from DSC and TGA

Samples	T_g / °C	**Weight loss temperature / °C**		$T_{Heat\text{-}resistance\ index}$*/ °C
		T_5	T_{30}	
Pure PI	205.6	505.8	585.5	271.3
1 wt% *f*-MWCNT-*g*-rGO/PI	206.3	508.3	590.5	273.2
3 wt% *f*-MWCNT-*g*-rGO/PI	209.5	515.1	597.2	276.5
5 wt% *f*-MWCNT-*g*-rGO/PI	211.8	517.2	620.5	283.8
10 wt% *f*-MWCNT-*g*-rGO/PI	216.2	519.5	632.4	287.7

References

1 T. Pi, K. Cole and J. Beck, *J. Heat Transf.-Trans. ASME,* 2017, **139**, 121301.

2 F. Yang and C. Dames, *Phys. Rev. B,* 2015, **91**, 165311.

3 S. Lepri, R. Livi and A. Politi, *Physics Reports-Review Section of Physics Letters*, 2003, **377**, 1-80.

4 C. W. Nan, R. Birringer, D. R. Clarke and H. Gleiter, *J. Appl. Phys.*, 1997, **81**, 6692-6699.

5 Y. Su, J. J. Li and G. J. Weng, *Carbon,* 2018, **137**, 222-233.

6 N. Bonfoh, A. Jeancolas, F. Dinzart, H. Sabar and M. Mihaluta, *Compos Struct,* 2018, **202**, 603-614.

7 M. Cao, C. Du, H. Guo, X. Li, S. Song, F. Tezel and B. Li,, *Compos. Pt. A-Appl. Sci. Manuf.*, 2018, **115**, 331-340.

8 S. Prolongo, R. Moriche, A. Urena, S. Florez, I. Gaztelumendi, C. Arribas and M. Prolongo, *J. Appl. Polym. Sci.,* 2018, **135**, 46475.

9 J. Yu, H. Choi, H. Kim and S. Kim, *Compos. Pt. A-Appl. Sci. Manuf.*, 2016, **88**, 79-85.

10 Y. Xiao, W. Wang, X. Chen, T. Lin, Y. Zhang, J. Yang, Y. Wang and Z. Zhou, *Compos. Pt. A-Appl. Sci. Manuf.*, 2016, **90**, 614-625.

11 I. Arief, S. Biswas and S. Bose, *ACS Appl. Mater. Interfaces*, 2017, **9**, 19202-19214.

12 W. Zhang, Z. Zhang, J. Yang, T. Huang, N. Zhang, X. Zheng, Y. Wang and Z. Zhou, *Carbon,* 2015, **90**, 242-254.